Paper

Int'l J. of Aeronautical & Space Sci. 15(1), 32–43 (2014)
DOI:10.5139/IJASS.2014.15.1.32

AFP mandrel development for composite aircraft fuselage skin

Deepak Kumar* and Myung-Gyun Ko**

Department of Aerospace Engineering, Gyeongsang National University, Jinju, Gyeongnam 660-701, South Korea

Rene Roy* and Jin-Hwe Kweon******

Department of Aerospace Engineering, Research Center for Aircraft Parts Technology, Gyeongsang National University, Jinju, Gyeongnam 660-701, South Korea

Jin-Ho Choi*****

School of Mechanical Engineering, Research Center for Aircraft Parts Technology, Gyeongsang National University, Jinju, Gyeongnam 660-701, South Korea

Soon-Kwan Jeong******

Korea Aerospace Industries, Yuceonri, Sanammyeon, Sacheon, Gyeongnam 664-942, South Korea

Jin-Woo Jeon*******

Dong-Hwa A.C.M, Jinyeongeup, Gimhae, Gyeongnam 621-801, South Korea

Jun-Su Han********

Gyeongnam Techno Park Aerospace Center, Bangjiri, Sanammyun, Sacheon, Gyeongnam 664-942, South Korea

Abstract

Automatic fiber placement (AFP) has become a popular processing technique for composites in the aerospace industry, due to its ability to place prepregs or tapes precisely in the exact position when complex parts are being manufactured. This paper presents the design, analysis, and manufacture of an AFP mandrel for composite aircraft fuselage skin fabrication. According to the design requirements, an AFP mandrel was developed and a numerical study was performed through the finite element method. Linear static load analyses were performed considering the mandrel structure self-weight and a 2940 N load from the AFP machine head. Modal analysis was also performed to determine the mandrel's natural frequencies. These analyses confirmed that the proposed mandrel meets the design requirements. A prototype mandrel was then manufactured and used to fabricate a composite fuselage skin. Material load tests were conducted on the AFP fuselage skin curved laminates, equivalent flat AFP, and hand layup laminates. The flat AFP and hand layup laminates showed almost identical strength results in tension and compression. Compared to hand layup, the flat AFP laminate modulus was 5.2% higher in tension and 12.6% lower in compression. The AFP curved laminates had an ultimate compressive strength of 1.6% to 8.7% higher than flat laminates. The FEM simulation predicted strengths were 4% higher in tension and 11% higher in compression than the flat laminate test results.

Key words: Composite, AFP, Mandrel, Fuselage, FEM

* Ph. D Candidate
** M.S.Student
*** Research Professor
**** Professor, Corresponding author: jhkweon@gnu.ac.kr
***** Professor
****** Deputy Senior Manager
******* Deputy Manager
******** Engineer

Received: February 21, 2014 Revised : March 5, 2014 Accepted: March 6, 2014

http://ijass.org pISSN: 2093-274x eISSN: 2093-2480

1. Introduction

In recent years, automated fiber placement (AFP) has become an important manufacturing technique used to fabricate complex composite parts that are widely applied in aviation and aerospace industries due to their advantages of high specific strength, high specific modulus, ablation resistance, and anti-corrosion, etc. [1]. AFP machines are a recent development of composite manufacturing technologies and are intended to increase rate and precision in the production of advanced composite parts. AFP machines place fiber reinforcements on a mold or mandrel in an automatic fashion and use a number of separate small width tows of thermoset or thermoplastic pre-impregnated materials to form composite layups [1]. One interesting feature of AFP is its use in constructing curvilinear fiber paths in order to optimize a composite structure [2]. In the aerospace industry, the manufacturing of large aircraft fuselage components is critical to minimize the number of joints. Russell et al. [3] described that large complex parts fabrication and high laydown rate demand for composite lay-ups in the aerospace industry motivated the need for machinery that can perform on-the-fly fiber placement at speeds of up to 50 meters per minute. Under such circumstances, composite structures can be competitive in terms of manufacturing cost through better material utilization and fewer joints, provided that the number of skin panels can be reduced. AFP is one of the automated production technologies that will enable this and similar manufacturing feats [4]. Several patent claims on this technology demonstrate the interest it generates. Clarke et al. [5] invented a device for automated composite layup on the inside of a cylindrical fuselage mandrel. This mandrel tool interior surface can therefore be manufactured to conform to the outside surface of the fuselage. Automated lay-up machines naturally allow material placement directly on an outside mold surface. Compared to manual prepreg placement, AFP allows greater control and accuracy in forming the exterior surface of the part; this results in fewer defects and higher surface quality compared to previously fabricated parts [6]. One of the problems with wrapping tape layers on the outside surface tool is that it is not possible to control the outside surface of the part, such as a fuselage section, without transferring the part to a female tool. Hanson [7] claimed a system design and a method to rapidly form and use a reconfigurable composite part mandrel, which can be applied to a composite aircraft fuselage. This reconfigurable mandrel is used to set the size, shape, and configuration of the composite part. In 2000, Benson et al. [8] invented a mandrel system that uses fiber placement machines that have multiple stands or rovings of fiber which are pulled from a creel assembly and placed onto the surface of a workpiece. The creel assembly controls the temperature of the spools and maintains the tension in the fibers. Application driven smart structures also combine advanced composite material fabrication techniques with embedding of relatively delicate fiber-optic sensors and piezo-actuators. Manufacturing a smart structure for a specific application requires the establishment of an integrated product design and manufacturing process [9, 10]. Measom et al. [11] reported that the use of AFP reduced the manufacturing cost of a tilt rotor aircraft rotor hub grip by over 60%. They also compared the mechanical properties of laminates prepared with AFP to those of other laminates made by conventional prepreg hand layup. Their measurements revealed that the AFP laminates had open-hole tensile and compressive strengths that were 6% lower than the hand layup laminates. Sawicki et al. [12] also tested AFP laminates in tension, compression, and shear for the development of an AFP fabricated aircraft fuselage. Compared to previous laminates made of prepreg tapes, they found that the AFP laminates had on average equivalent or better strength and modulus. They found that the greatest improvement was in compression, where the AFP laminates had a 7.3% strength improvement.

In this paper, an AFP mandrel for a composite aircraft fuselage was designed and developed according to design requirements and constraints. Finite element modeling (FEM) and modal analysis were performed to accurately predict the deflection and natural frequency of the mandrel. The analysis was also performed to predict the stress and displacement due to the load from the AFP head and the structure self-weight. A thermal analysis simulation was also conducted, considering the projected composite curing temperature. Finally, the mandrel was manufactured, and a prototype carbon/epoxy composite fuselage skin was fabricated with the AFP process. Additionally, experimental tensile and compressive tests were performed on the fuselage skin for different specimens (curved and flat AFP laminates), in order to evaluate its mechanical properties. The test results were also validated with FEM numerical simulations.

2. Mandrel design

In the AFP process applied to the aircraft fuselage fabrication, a fiber placement head deposits bundles of fibers (“tows”) onto a rotating mandrel tool. The tows are narrower and more easily manipulated than prepreg tapes. AFP is most effective when placing material on a curved or contoured surface [13]. A system comprises an automated fiber placement (AFP) machine and a layup mandrel tool supported by the AFP machine. The mandrel geometry is designed such that the mandrel can sustain its self-weight and the load from the AFP head. For the aircraft fuselage skin studied, the mandrel was designed such that the shape should be tapered cylindrically. The maximum weight of the mandrel was set at 18 tons. The maximum center deflection of the mandrel should be below 1 mm and the minimum natural frequency of the mandrel should be higher than 15 Hz (design limits).

The proposed mandrel is composed of a tapered steel cylinder with attachment parts, and the cylinder has panels (barrel) which have stiffeners and ribs, as shown in Fig. 1. The attachment parts are designed such that they can grip properly to the AFP machine heads. The attachment parts include numerous pocket holes, symmetrically repeated, which are attached to the mandrel barrel with fasteners. Provisions are taken so that the AFP machine spindle can extend through the attachment part and mandrel barrel. The mandrel panel herein provides a layup surface for the fuselage skin. It has a stiffening support structure to ensure that the surface panels have the necessary stiffness during fiber placement. The stiffening support structure interfaces the mandrel panel with ribs. The stiffening support structure permits minimum displacement when the fiber placement head makes contact with the panel, in order to avoid the formation of dimples and wrinkles. The dimensions of the stiffening support structure and the ribs are a function of the strength and deflection requirements. Stiffeners and ribs also contribute to damp vibrations during fiber placement. The vibrations result from two main sources: periodic contact of the fiber placement head and angular acceleration of an extremely large steel structure.

The thickness of the ribs and stiffeners are 25 mm and 30 mm, respectively. The relative distance between longitudinal ribs is 348 mm (mandrel circumference-wise), and 640 mm for circumferential stiffeners (mandrel longitudinal-wise). The total length of the mandrel surface panel is 4 m and its thickness is 15 mm. The outer diameter of the mandrel is 2.2 m on one side and 1.8 m on the other side. Ridges between the plates are designed to provide additional vibration damping. The AFP machine spindle and mounting details should not affect the vibration frequency of the mandrel. The material for the mandrel was selected as SS400 structural steel (Table 1).

Table 1. Material properties of structural steel 400.

Elastic modulus – E (Gpa)	205
Poisson's ratio – ν	0.29
Yield strength – σ_y (MPa)	245
Density – ρ (kg/m^3)	7850
Coefficient of thermal expansion (m/m/°C)	15 x10^{-6}

3. Finite element model

The initial design of the mandrel was partially based on a number of simplified analytical calculations. To investigate the validity of the designed mandrel, a finite element simulation using the MSC Nastran commercial FEM code was carried out. The mandrel geometry was created with the CATIA v5 CAD software. The CATIA model was imported in MSC Patran (pre & post processor) and solved in MSC Nastran (Solver). For the model meshing, tetrahedral 10 solid elements (Tet10) were used. The final number of elements in the model was determined after deflection and stress convergence testing. Convergence testing was performed to evaluate if the mesh is refined enough to obtain a solution that can be trusted. The model used for analysis had a total

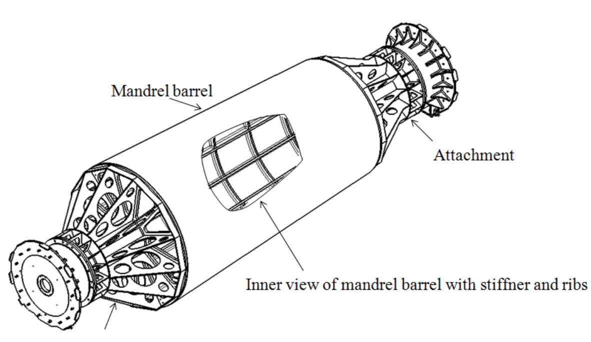

Fig. 1. Schematic view of mandrel assembly for AFP.

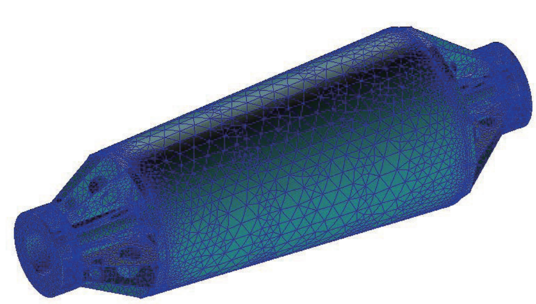

Fig. 2. Three-dimensional finite element model for mandrel (125,500 elements).

of 125,500 elements and 251,763 nodes. This finite element model is shown in Fig. 2. The effect of gravity was also considered, and the acceleration value was taken as 1.5*g (14.7 m/s^2), where g is the acceleration due to gravity and a 1.5 margin of safety.

Three static load cases were studied: a) structure self-weight, b) structure self-weight and a 2940 N (300 kg) concentrated load at the center, and c) structure self-weight and a 2940 N (300 kg) load distributed over a 50 mm wide region at the center. The mandrel attachment parts were kept fixed on both sides (Fig. 3). The concentrated load in case (b) may represent an irregular sharp contact of the AFP head on the mandrel, while the distributed load in case (c) aims to represent a more realistic load distribution from the AFP head. The 50 mm width used in case (c) represents the shortest distance between two nodes for the mesh dimension used. In addition to this analysis, the effect of temperature on the mandrel was also studied. A curing temperature of 180 °C was considered, in order to check thermal deformations of the mandrel during the curing process. The initial temperature was taken as the room temperature, 25 °C (ΔT= 155°C). A linear modal analysis was also performed in MSC Nastran using the Lanczos extraction method.

4. Finite element results and discussion

The maximum static deformations for the three load cases occurred in the attachment region, and were computed as 0.0966 mm (case a), 0.0981 mm (case b), and 0.0995 mm (case c). The maximum deflections in the middle of the mandrel barrel were 0.0745 mm (case a), 0.0767 mm (case b), and 0.0782 mm (case c). Load case (c) was found to be the most critical and is shown in Fig. 4. The deformation found in the region of interest (mandrel barrel) is within the design limit (< 1 mm). Maximum von Mises stresses were found as 22 MPa (case a), 23.3 MPa (case b), and 23.3 MPa (case c). These maximum stresses were found in the attachment part of the mandrel and they were judged to be not critical because they are much lower than the yield strength of the steel (245 MPa). The stress plot for load case (c) is shown in Fig. 5. Maximum deformation in the longitudinal direction due to cure temperature is computed as 4.99 mm, and is shown in Fig. 6. In the circumferential direction, the maximum thermal deformation is 6.06 mm at the largest diameter (2.2 m → 2.20606 m). The minimum natural frequency of the AFP mandrel was computed as 40.00 Hz, which is within the design limit (> 15 Hz). Table 2 lists the different mode frequency values obtained through modal analysis in the MSC Nastran code.

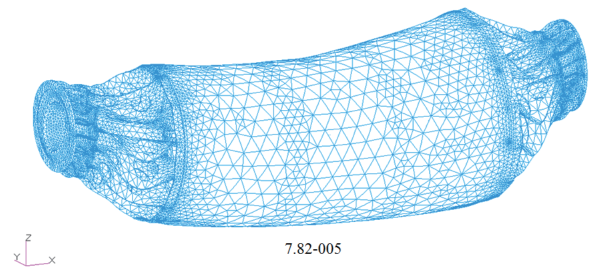

Fig. 4. Deformed shape of mandrel (load case 3) (unit: m).

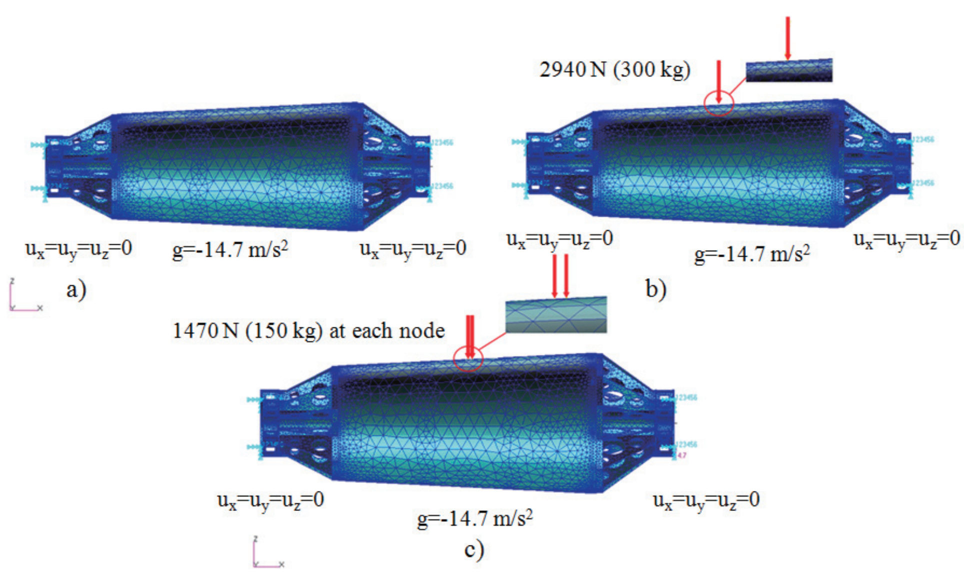

Fig. 3. FEM boundary conditions: a) self-weight case, b) self-weight and 2940 N (300 kg) concentrated load case, c) self-weight and 2940 N (300 kg) distributed load case.

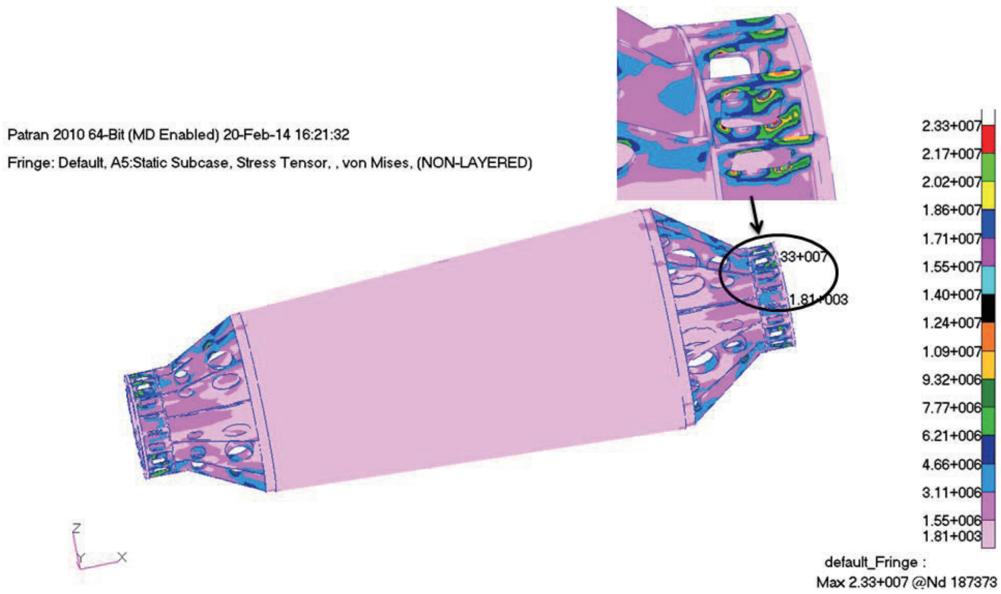

Fig. 5. von Mises stress plot (load case 3) (unit: Pa).

Fig. 6. Displacement in x-direction by thermal load during autoclave curing (unit: m).

Table 2. Normal modes and natural frequencies.

Mode number	1	2	3	4	5
Natural frequency (Hz)	40.00	86.14	86.19	127.3	130.7

5. Composite fuselage skin development

The designed mandrel was manufactured. The AFP manufacturing set-up and manufactured mandrel are shown in Fig. 7 and Fig. 8. In the fuselage skin design phase, the skin thickness and ply angle configuration should first be determined. Denis Howe [14] suggested equations for an initial design approach to estimate the skin thickness. He stated that the condition of pressurized skin should first be considered. According to this method, the thickness of the skin to resist pressurization is derived from,

$$t_p = \frac{P.R}{\sigma_P} \tag{1}$$

where P is the pressure differential, R is the radius of the fuselage shell, and σ_p is the allowable tensile working stress of the skin. This is analogous to the case of a pressurized thin walled cylinder.

The skin thickness to resist a bending moment can be calculated from,

$$t_e = \frac{M}{\sigma_a A} \tag{2}$$

where M is the bending moment, A is the area enclosed by the fuselage cross section, and σ_a is the allowable bending stress of the skin.

The skin thickness to resist torsion shear can be calculated from,

$$t_q = \frac{T}{2A\sigma_s} \tag{3}$$

where T is the applied ultimate torque and σ_s is the allowable shear stress of the skin.

A prototype fuselage was fabricated in order to test the mandrel, the AFP fabrication process, and the characteristics of the fabricated part. The fuselage skin was made of carbon fiber/epoxy resin prepreg tows (BMS276 [15], TY/35, Class 7, Grade 170) with a laminate stacking sequence of $[45/90/-45/0/45/0/-45]_s$, giving a total thickness of 2.667 mm. This fuselage skin configuration was chosen as a first iteration for the process development and is not optimized for an actual aircraft design case. For example, using equation (1) with P=0.7bar, σ_p=197.8 MPa (from FEM as in section 7.3), R=1.1 m, and a safety factor of 1.5, we obtain t_p=0.58 mm. The AFP machine used was from Mtorres (M.Torres Disenos Industriales S.A., Navarra, Spain). Two days were required, including preparation time, to lay the skin material on the mandrel. Vacuum bagging was then applied on the skin layup. The part was cured for 8 hours in an autoclave oven, with a maximum cure temperature of 180 °C and a maximum pressure of 9 atm. Fig. 8 shows the configuration of the fabricated fuselage skin. The fuselage section is 3 m long and tapered so that the diameter of one side is 1.8 m and that of the other side is 2.2 m.

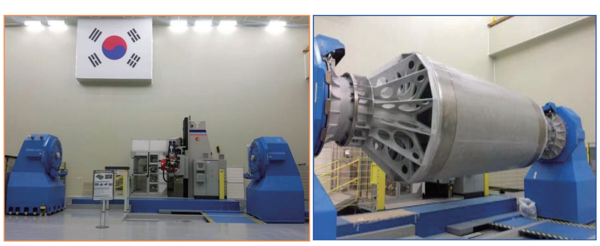

Fig. 7. AFP machine (left) and installed mandrel (right).

Fig. 8. Composite fuselage skin manufactured using AFP.

6. Fuselage skin mechanical property test

Tests were performed to measure the ultimate strength and elastic modulus of AFP manufactured laminates under tensile and compressive loading. Fig. 9 shows the position of specimens selected directly from the fuselage skin. Since the fuselage shape is tapered, these specimens were slightly curved to a varying degree depending on their position on the fuselage. Similar laminate specimens made by AFP, this time on a flat mold surface, were also prepared and tested. Additionally, specimens taken from a laminate made by a prepreg (BMS8-276) hand layup, with the same material and stacking sequence, were also prepared and tested for comparison. The scale of the specimen geometry was chosen in order for the test to be representative of the target structure (fuselage skin), and to comply with ASTM test standards. The main direction (0°) of the test specimen was in the fuselage longitudinal direction. The AFP specimen's geometry is shown in Fig. 10 for the tests considered. The specimen shapes were chosen considering the fuselage geometry, so that the material strength of the curved and flat laminates could be compared. The specimen dimensions were 250 mm x 25 mm for the tensile test and 140 mm x 25 mm for the compressive test. Curved and AFP flat specimens

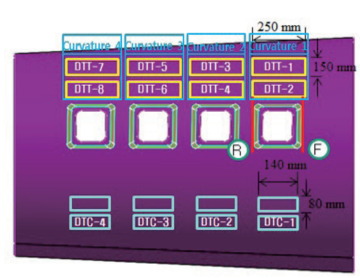

Fig. 9. Position of test specimens for mechanical property evaluation.

were coded as DTT (AFP tensile curved), CPTL (AFP tensile flat), DTC (AFP compressive curved), and CPCL (AFP compressive flat). Four specimens were tested for each case. The effect of curvature on the specimen geometry was small enough that no special measures were taken in the tests. For the tensile curved specimens, tabs were installed in the same fashion as flat specimens. The tab adhesive thickness served to accommodate the specimen's minor curvature. Fig. 11

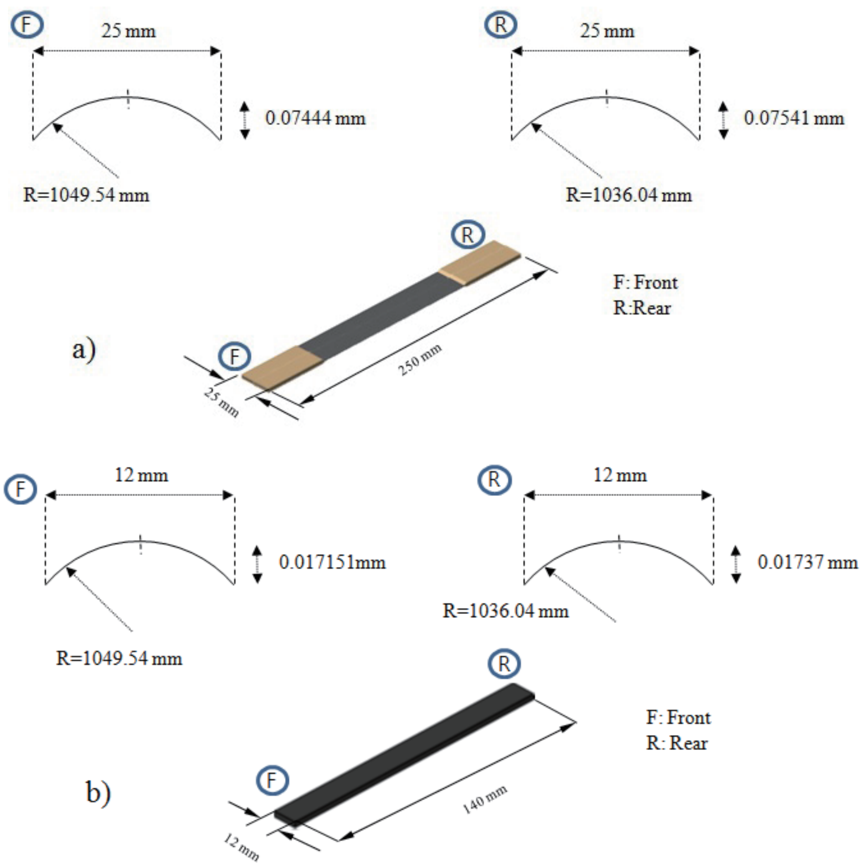

Fig. 10. Curved test specimen geometry: a) tensile specimen (DTT1), b) compressive specimen (DTC1).

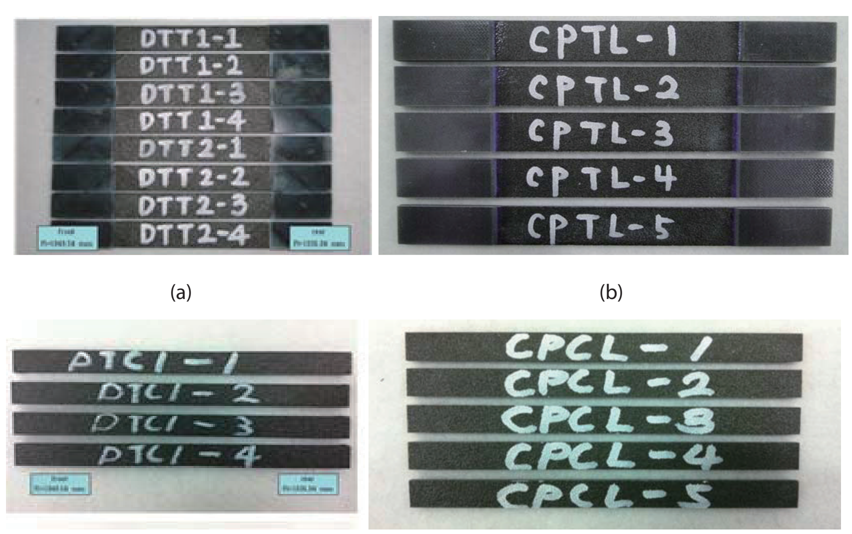

(a) (b)

(c) (d)

Fig. 11. Test specimens: a) tensile tests (curved), b) tensile tests (AFP flat), c) compressive tests (curved), d) compressive tests (AFP flat).

shows the prepared test specimens for the considered cases.

Tensile testing was performed according to ASTM D3039 [16] and compression testing was performed according to ASTM D6641 [17]. Fig. 12 shows the experimental set-ups. All compression and tensile tests were conducted at our lab using a servo-hydraulic universal test machine, model Instron 5582 (Illinois Tool Works Inc., Norwood, USA), with a digital controller and data acquisition. Tests were conducted using a constant head displacement rate of 2 mm/minute in tension and 1.3 mm/minute in compression. For all specimens, a 90° 2-element cross polyamide backed strain gage (Tokyo Sokki Kenkyujo co. Ltd) with 3 mm gage length and 120 Ω resistance was used for strain measurements. Strain measurements were made using a measurement strain conditioner and amplifier system, interfaced with the universal test machine for simultaneous data acquisition of load, stroke, and strain, recorded 5 times per second.

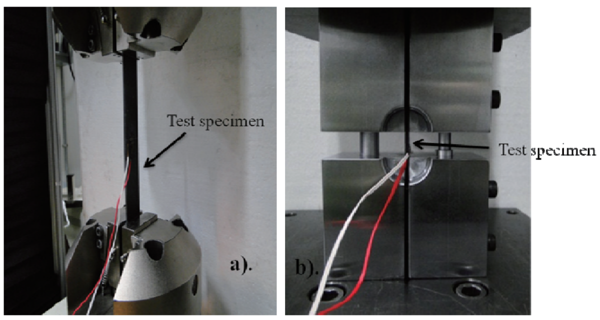

Fig. 12. Test set-up: a) tensile test, b) compressive test.

7. Mechanical property test results and discussion

7.1 Tensile test results

Fig. 13a and Fig. 13b show the stress strain behavior of specimens under tensile loading, which is mainly elastic linear. The elastic modulus was calculated according to ASTM D3039 [16] in the strain interval of 1000~3000 μm. The ultimate strength was taken as the highest sustained load divided by the initial specimen section area. Average values of elastic modulus and ultimate strength were calculated for every specimen type, as shown in Fig. 14. The error bars in the chart represent the range limits of the results. The average ultimate tensile strengths of the curved

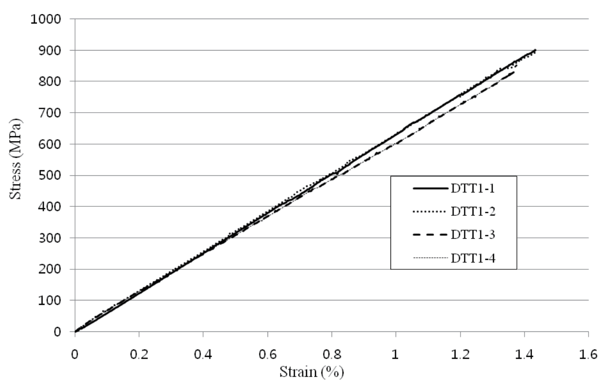

a) Tensile test for AFP curved specimens (DTT1)

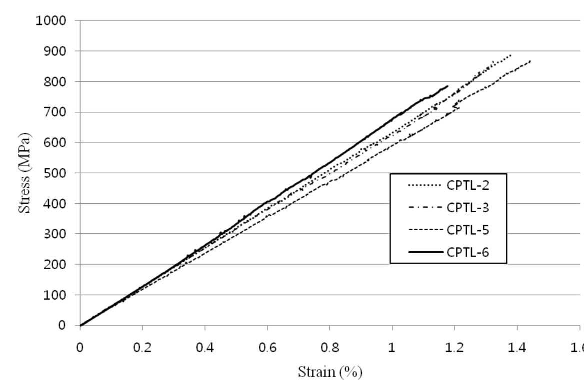

b) Tensile test for AFP flat specimens (CPTL)

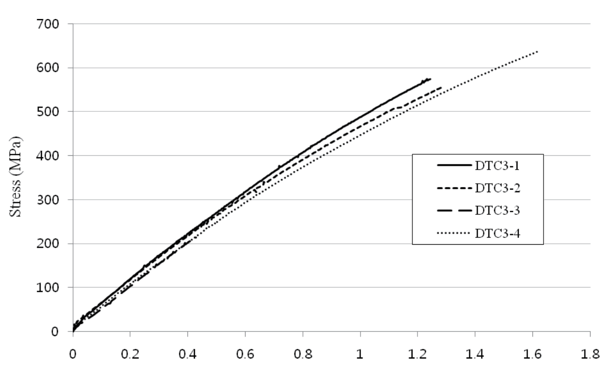

c) Compressive test for AFP curved specimens (DTC3)

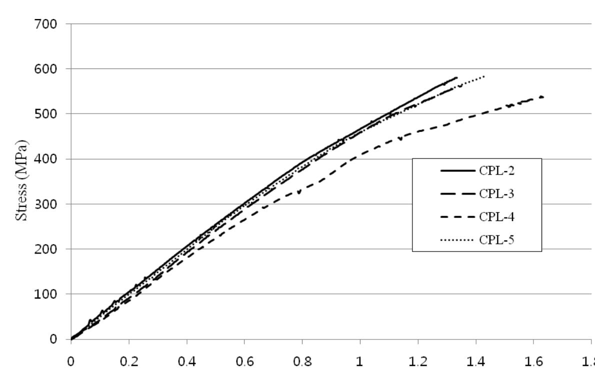

d) Compressive test for AFP flat specimens (CPCL)

Fig. 13. Stress- strain plots.

AFP fabricated specimens ranged from 835.4 MPa to 880.1 MPa. This compares to a strength of 870.8 MPa for the flat AFP specimens. For the first three curved specimen groups, with a curve radius range of 980 – 1049 mm, the average strength is close to that of the flat AFP specimens. The fourth group, with the lowest curvature radius (r= 953 ~ 971 mm), has a slightly lower average strength compared to the flat AFP laminates (-4.06%). The average measured tensile moduli were in the range of 58.7 – 62.8 GPa for the curved AFP specimens, compared to 62.9 GPa for the flat AFP specimens. The moduli of the curved AFP specimens were thus slightly lower than those of the flat AFP specimens (-0.2% to -6.7%). The average values of Poisson's ratio for curved AFP specimens ranged from 0.44 to 0.47, compared to 0.45 for the flat AFP specimens. In the case of the hand layup specimens, their average ultimate tensile strength was 871.9 MPa, and this is comparable to that of the AFP specimens. Only the AFP specimen group with the most pronounced curve has a slightly lower strength (835.4 MPa). The hand layup specimen's tensile modulus (59.8 GPa) and Poisson's ratio (0.46) are also comparable to the AFP specimens. It was therefore observed that the tensile ultimate strength, elastic modulus and Poisson's ratio for different curved parts of the fuselage skin showed almost equal values compared to the flat AFP and hand layup laminates. In comparison, Poon [18] tested un-notched [45/0/-45/90]6S CFRP laminates in tension and obtained an average ultimate strength of 827 MPa and an elastic modulus of 57.9 GPa.

7.2 Compressive test results

Fig. 13c and Fig. 13d show the stress-displacement and stress-strain behavior of specimens under compressive loading. For the curved and flat AFP specimens, the stress-strain behavior showed slightly more deviation from linearity. The elastic modulus was calculated according to ASTM D3410 [19] in the strain interval of 1000~3000 μm. The ultimate strength was taken as the highest sustained load divided by the initial specimen section area. Average values of elastic modulus and ultimate strength were calculated for curved and flat AFP laminates, as shown in Fig. 15. The

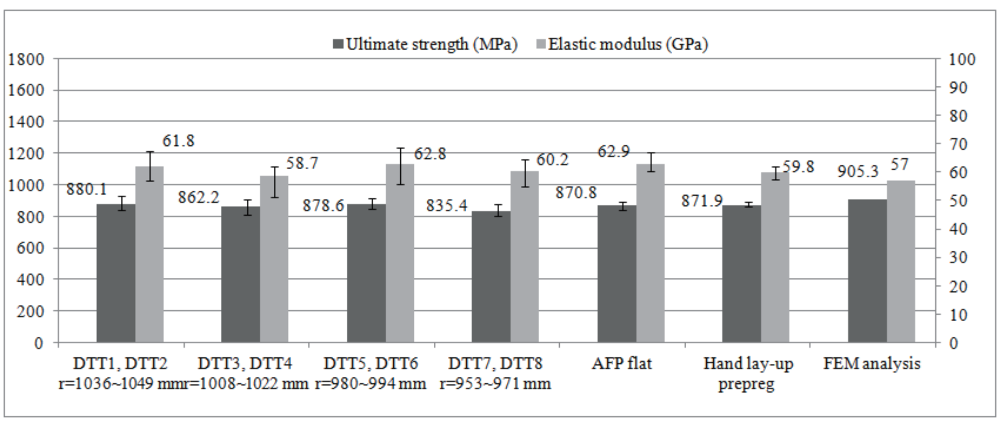

Fig. 14. Comparison of test and finite element results (tensile).

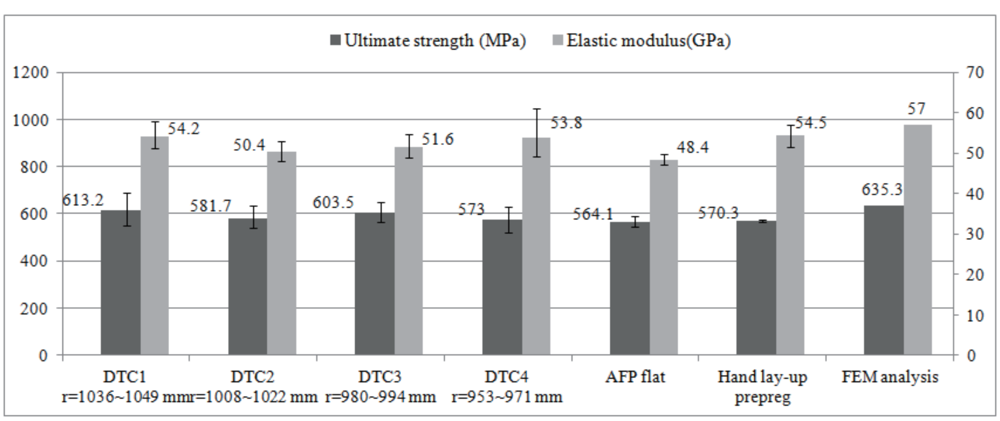

Fig. 15. Comparison of test and finite element results (compressive).

average ultimate compressive strengths of curved, AFP fabricated specimens, range from 573.0 MPa to 613.2 MPa. This compares to a strength of 564.1 MPa for the flat AFP laminate specimens. The curved specimens therefore had a higher average ultimate compressive strength than flat AFP specimens, with an improvement range of 1.6% to 8.7%. There was no clear indication that this improvement was a function of the curvature radius amplitude. In the case of the hand layup specimens, their average ultimate compressive strength was 570.3 MPa, and this is also comparable to the AFP specimens. For comparison, Soutis [20] had also tested [0/±45/0/90/0/±45/0/90/0/±45/0]S laminates in compression and measured an average ultimate strength of 646 MPa. The average measured compressive moduli in the present tests were in the range of 50.4 – 54.2 GPa for the curved specimens, compared to 48.4 GPa for flat AFP specimens. The curved specimens therefore had an average compressive modulus which was 4.1% to 12.0% higher than that of the flat AFP specimens. Again there was no clear indication that this improvement was a function of the curvature radius amplitude. The compressive modulus (54.5 GPa) of the hand layup specimen is also comparable to that of the AFP specimens. The average measured values of Poisson's ratio for curved specimens were all 0.41, while no valid measurement was made for flat AFP and hand layup specimens. The compressive-to-tensile strength ratio(x) was in the range of 0.67 to 0.70 for curved AFP specimens, compared to 0.65 for flat AFP specimens. Microscope observations and image analysis also revealed no significant porosity in all AFP fuselage skin laminates. This absence of porosity and the comparative strength results (AFP versus hand layup laminates) are indications that the AFP process with this mandrel produces good quality laminates.

7.3 Comparison of measured and predicted mechanical properties

A finite element analysis of the test specimens was conducted for tensile and compressive loading with MSC Nastran v2010. The finite element model was used in such a way as to replicate the test conditions. The details of material properties used are listed in Table 3. A linear orthotropic material model was used to define the laminate properties, defined by elastic moduli E_{11} and E_{22}, Poisson's ratio ν_{12}, and shear modulus G_{12}. The specimen geometry was created in MSC Patran. Models were meshed with 4-node shell elements (CQUAD) with the laminate option, where the definition of each ply is implemented [23]. A maximum stress failure criterion was used. One side of the test specimen was kept fixed and a load was equally distributed on the other side. The finite element models are shown in Fig. 16a and Fig. 17a. A linear static analysis solution was performed and the load corresponding to a failure index of 1 was determined by trial and error. Matrix failure (cracking) was first observed in tension for the 90° and ±45° plies. This was not considered as the ultimate failure, since the 0° plies still had not failed in their fiber

Table 3. CFRP material properties: BMS276, TY/35, Class 7, Grade 170 (Toray Industries, Inc.).

Property	Unidirectional AFP lamina	Laminate effective properties [21]
Elastic modulus – E_{11} (GPa)	141	57.0
Elastic modulus – E_{22} (GPa)	8.95	40.5
Shear modulus – G_{12} (GPa)	2.59	22.5
Poisson's ratio – ν_{12}	0.32	0.45
Tensile strength – F_{11t} (MPa)	2580	–
Tensile strength – F_{22t} (MPa)	46.2	–
Compressive strength[1] – F_{11c} (MPa)	2110	–
Compressive strength[1] – F_{22c} (MPa)	206.8	–
Thermal expansion – $CTE_{1(0°)}$ [22] (m/m/°C)	0.21×10^{-6}	1.44×10^{-6}
Thermal expansion – $CTE_{2(90°)}$ [22] (m/m/°C)	29.8×10^{-6}	3.18×10^{-6}

[1]: Manufacturer-provided data

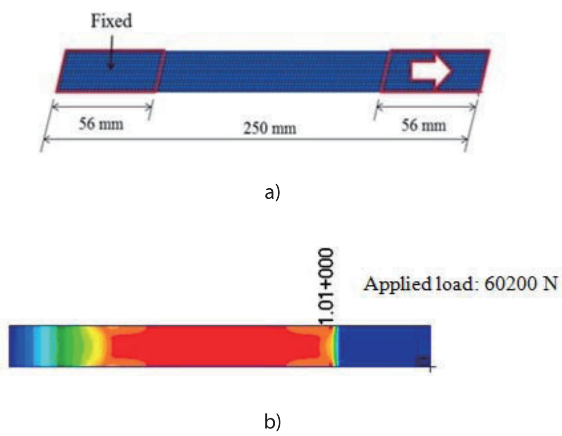

Fig. 16. Tensile test: a) finite element model, b) failure index corresponding to maximum applied load.

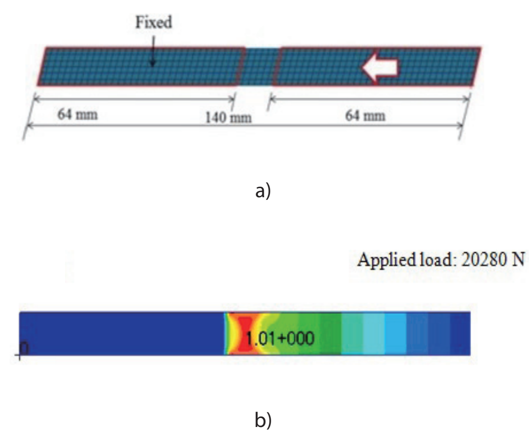

Fig. 17. Compressive test: a) finite element model, b) failure index corresponding to maximum applied load.

direction. Reduced ply properties were then used for the cracked 90° and ±45° plies, based on [24]: $\overline{E_{22}}$=0.27.E_{22}, $\overline{G_{12}}$=0.45. G_{12}.The results showed that the failure load for the tensile case (Fig. 16b) was 60.2 kN, corresponding to 905.3 MPa. For the compressive case (Fig.17b), the failure load was 20.3 kN, corresponding to 635.3 MPa. These simulation results are compared to the test results in Fig. 13 and Fig. 14. The simulation result would suggest a strength of around 4% (tension) and 11% (compression) higher than the flat specimens test result. Nonetheless, the simulation result is at the upper range limit of the variation interval of the test result, so the agreement can be satisfactory.

8. Conclusion

In this work, the design of an AFP mandrel for aircraft composite fuselage skin fabrication was presented. In order to verify the mandrel's deformation under operation and its vibration characteristics, finite element modeling was performed. The maximum static deformation (d_{max}) and stress (σ_{max}) were found within the chosen design limit: d_{max}= 0.0995 mm < 1 mm, and σ_{max}=23.3 MPa < σ_y=245 MPa. The maximum deflection in the middle of the mandrel barrel was also found as 0.0782 mm. The simulated mandrel lowest natural frequency (ω_{min}) was also higher than the chosen design criteria: ω_{min}=40.0 Hz > 15 Hz. The mandrel deformation due to curing temperature was also studied. The designed AFP mandrel was manufactured. A prototype composite fuselage skin was fabricated and material samples were taken from it and tested in tension and compression loading. Material ultimate strength and elastic modulus were measured for curved specimens (from the fuselage) and compared to specimens taken from equivalent flat AFP and hand layup laminates. The measurements were then validated with FEM results. The flat AFP and hand layup specimens showed almost identical tensile and compressive strengths. For different levels of specimen curvature, the average ultimate compressive strength was 8.7%, 3.1%, 7.0% and 1.6% higher than flat specimens. Under tensile loading, the different curved specimen's average ultimate tensile strength difference compared to non-curved specimens was 1.90%, 4.65%, -0.137%, and 3.34%. The laminate ultimate strength from FEM simulation results was found to be 4% higher in tension and 11% higher in compression than the flat specimen test results. This work showed that the strength and modulus of a fuselage composite skin laminate fabricated with automated fiber placement (AFP) can be comparable to a laminate fabricated from a conventional prepreg hand layup. We believe the application of AFP offers notable advantages in terms of manufacturing workforce reduction and the precision and repeatability of composite ply placement.

Acknowledgement

This work was supported by the Priority Research Centers Program through the National Research Foundation of Korea (NRF) funded by the Ministry of Education, Science and Technology (2009-0094104). This research was financially supported by the Ministry Of Trade, Industry & Energy (MOTIE), Korea Institute for Advancement of Technology (KIAT) and Dong-Nam Institute For Regional Program Evaluation (IRPE) through the Leading Industry Development for Economic Region.

References

[1] Hinrichsen, J. and Bautista, C., "The challenge of Reducing both Airframe Weight and Manufacturing Cost", *Air & Space Europe*, Vol. 3, Issue 3-4, 2001, pp. 119-121.

[2] Croft, K., Lessard, L., Pasini, D., Hojjati, M., Chen, J. and Yousefpour, A., "Experimental Study of the Automated Fiber Placement Induced Defects on Performance of Composite Laminates", *Composites Part A*, Vol. 42, Issue 5, 2011, pp. 484-491.

[3] Russel, D., Kyle, J. and Peter, V., "High-Speed Fiber Placement on Large Complex Structures", *SAE international*, 2007-01-3843.

[4] John, M., "Applying Automation to the Fabrication of Composite based Aerospace Parts and Developing a Machine Specification", Accudyne Systems Inc., USA.

[5] Clarke, R. R., Engwall L.D., Yonash G. M. and New, A. J., "Unidirectional, Multi- head Fiber Placement", United States patent 7048024 B2, 2005.

[6] Engwall L. D., Yonash, G. M., Clark R. R. and New, A. J., "Automated Composite Lay-up to an Internal Fuselage Mandrel", United States patent 7083698B2, 2006.

[7] Hanson F. S., "Rapid Reconfigurable Fuselage Mandrel", United States patent 7648661 B2, 2010.

[8] Benson M. V., Gill, R.D., Nielsen P.J., Mansouri, H. and Shepherd, I. N., "Multiple Axes Fiber Placement Machine", United States patent 6096164, 2000.

[9] Thomas M. M., Glowasky A. R., Mcllroy E. B. and Story A.T., "Manufacturing of Smart Structures using Fiber Placement Manufacturing Processes", *266/SPIE*, Vol. 2447, 1995, pp. 266-273.

[10] Farinelli, C., Kim, H.-I. and Han, J.-H., "Feasibility Study to Actively Compensate Deformations of Composite Structure in a Space Environment", *International Journal of Aeronautical Space Sciences*, Vol. 13, No. 2, 2012, pp. 221-228.

[11] Measom, R. and Sewell, K., "Fiber Placement Low-cost Production for Complex Composite Structures", *Proceedings of the American helicopter society 52nd annual forum*, Washington DC, USA, 1996.

[12] Sawicki, A., Schulze, E., Fitzwater, L. and Harris, K., "Structural Qualification of V-22 EMD Tow-placed Aft Fuselage", *Proceedings of the American helicopter society 51st annual forum*, Fort Worth TX, USA, 1995, pp. 1641-1653.

[13] Simon, S., Mostafa, R., "Automated Fiber Placement including Layup Mandrel Tool", European patent 2631062 A1, 2013.

[14] Howe, D., *Aircraft Loading and Structural Layout*, Professional Engineering Publishing, London, 2004.

[15] Boeing Material Specification, "BMS 276 Advanced Composites – 350°F Cure Toughened – epoxy Pre-impregnated Carbon Fiber Tapes and Fabrics", Boeing Corporation, Chicago, USA.

[16] Standard Test Method for Tensile Properties of Polymer Matrix Composite Materials, ASTM Standard D3039/D 3039M.

[17] Standard Test Method for Determining the Compressive Properties of Polymer Matrix Composite Laminates Using a Combined Loading Compression (CLC) Test Fixture, ASTM Standard D6641 / D6641 M.

[18] Poon, C., "Tensile fracture of notched laminates", National Research Council of Canada, 1991.

[19] Standard Test Method for Compressive Properties of Polymer Matrix Composite Materials With Unsupported Gage Section by Shear Loading, ASTM Standard D3410/D3410M.

[20] Soutis, C., "Compressive Fracture of Orthotropic Laminates containing Open Holes due to Fibre Micro-instability", *Proceedings of ICF 10*, Honolulu, USA, 2001.

[21] Jones, R. M., *Mechanics of Composite Materials*, Taylor & Francis, New-York, 1999.

[22] Nawab, T., Jacquemin, F., Casari, P., Boyard, N., Borjon-Piron, Y. and Sobotka, V., "Study of Variation of Thermal Expansion Coefficients in Carbon/Epoxy Laminated Composite Plates", *Composites Part B*, Vol. 50, July 2013, pp. 144-149.

[23] Park, Y.-B., Nguyen, K.H., Kweon, J.-H., Choi, J.-H. and Han, J.-S., "Structural Analysis of a Composite Target-drone", *International Journal of Aeronautical Space Sciences*, Vol. 12, No. 1, 2011, pp. 84-91.

[24] Noh, J. and Whitcomb, J., "Effect of Various Parameters on the Effective Properties of a Cracked Ply", *Journal of composite materials*, Vol. 35, Issue 8, 2001, pp. 689-712.